The Impact of Land Use Change on the Hydrological Response in a Mountainous Watershed Using the SCS-CN Model

Ziana Ziana
Department of Civil Engineering, Universitas Syiah Kuala, Banda Aceh, Indonesia
ziana@usk.ac.id (corresponding author)

Muhammad Asyifa' An-Nur
Department of Civil Engineering, Universitas Syiah Kuala, Banda Aceh, Indonesia
nur.b20@mhs.usk.ac.id

Cut Dwi Refika
Department of Civil Engineering, Universitas Syiah Kuala, Banda Aceh, Indonesia
cut.dwi.refika@usk.ac.id

Mubarak Mubarak
Department of Civil Engineering, Universitas Syiah Kuala, Banda Aceh, Indonesia
mubarak@usk.ac.id

Received: 13 January 2026 | Revised: 19 February 2026 and 27 March 2026 | Accepted: 3 April 2026

ABSTRACT

The Geuni Watershed, a sub-basin of the Meureudu Watershed, has experienced recurrent flooding in recent years, indicating increasing hydrological vulnerability in mountainous tropical catchments. This study quantifies the effects of land-cover change and Watershed characteristics on flood discharge in the Geuni Watershed using a hydrological modeling approach. The Soil Conservation Service–Curve Number (SCS–CN) method was used to estimate direct runoff under different land-use scenarios, and spatial analysis was conducted using Geographic Information Systems (GIS). Rainfall data were processed to derive design storm events, and morphometric parameters were analyzed to evaluate Watershed response characteristics. The results indicate no significant increase in Curve Number (CN) values in areas where forest and mixed vegetation are converted to agricultural land and settlements. Steep topography and a relatively short time of concentration further intensify peak flow generation, leading to rapid flood onset in downstream areas. The findings demonstrate that flood occurrences in the Geuni Watershed are driven by the combined effects of high-intensity rainfall, unfavorable morphometric characteristics, and anthropogenic land-cover alteration. Within the Meureudu basin system, hydrological disturbances in the Geuni Subwatershed cumulatively contribute to basin-scale flood risk. The study highlights the need for integrated Watershed management strategies, including upstream conservation, reforestation, soil and water conservation measures, and land-use control to mitigate future flood hazards. The proposed approach provides an engineering-oriented, spatially explicit framework suitable for flood risk assessment in comparable tropical mountainous Watersheds.

Keywords-land-use change; flood discharge; mountainous watershed; SCS-CN; hydrological response

I. INTRODUCTION

Flood events are among the most frequent natural hazards in tropical regions, particularly in mountainous Watersheds, where topographic and climatic factors strongly shape hydrological processes. Steep slopes, high rainfall intensity, and limited soil storage capacity produce rapid runoff and short concentration times, resulting in higher peak discharges than in lowland areas. Consequently, mountainous catchments are highly sensitive to hydrological extremes due to their rapid response and limited buffering capacity [1].

Recent studies indicate that Watershed hydrological responses are not solely governed by climatic inputs but are also significantly influenced by land-use and land-cover (LULC) changes driven by human activities. These changes alter key components of the hydrological cycle, including streamflow, evapotranspiration, and runoff generation, thereby modifying the rainfall–runoff relationship in a catchment [2]. Land-use change, such as deforestation, agricultural expansion, and urban development, reduces vegetation cover and interception capacity and limits soil infiltration, ultimately increasing surface runoff and peak discharge [3]. Empirical evidence further shows that converting forested areas to agricultural or built-up land significantly increases runoff coefficients and flood potential, particularly in environmentally sensitive regions [4].

Understanding the relationship between land-cover dynamics and hydrological response is essential for effective Watershed management and flood-mitigation planning. The Krueng Meureudu Watershed in Aceh Province, Indonesia, features mountainous upstream areas and relatively narrow downstream channels. One of its important Subwatersheds, the Geuni Watershed, has experienced recurrent flooding in recent years, driven by high rainfall intensity and rapid runoff responses from steep upstream regions. In addition, LULC changes in the upstream area, particularly the conversion of forest land to agricultural land and settlements, have altered the hydrological response by reducing infiltration capacity and increasing surface runoff, thereby elevating flood risk in downstream areas.

Hydrological modeling is essential for analyzing Watershed responses to rainfall and land-surface changes. A range of modeling approaches has been developed, from physically based to empirical models. Among these, the SCS–CN method is widely used for its simplicity, relatively low data requirements, and ability to incorporate land use and soil characteristics into runoff estimation [5, 6]. The method estimates direct runoff as a function of rainfall, soil properties, land cover, and antecedent moisture conditions, making it suitable for practical Watershed applications [6].

The SCS–CN method expresses direct runoff as:

$$Q = \frac{(P-I_a)^2}{P-I_a+S}, P > I_a \tag{1}$$

where Q is runoff depth, $P$is rainfall, I_a is initial abstraction, and S is potential maximum retention. The parameter S is related to the CN by

$$S = \frac{25400}{CN} - 254 \tag{2}$$

with $I_a = 0.2S$. The CN value represents Watershed runoff potential and depends on land cover, soil type, and antecedent moisture condition [5, 6].

For peak discharge estimation, the SCS Unit Hydrograph (SCS-UH) method is commonly used in conjunction with the SCS–CN approach [6, 7].

Peak discharge is estimated as:

$$Q_p = \frac{0.208 \cdot A \cdot Q}{T_p} \tag{3}$$

where A is watershed area, Q is runoff depth, and T_p is time to peak.

The time to peak is defined as:

$$T_p = T_{lag} + \frac{D}{2} \tag{4}$$

with basin lag time approximated as: $T_{lag} = 0.6 \cdot T_c$

where T_c is the time of concentration [6].

Despite its widespread use, the SCS–CN method has several limitations in mountainous Watersheds. Many studies rely on lumped parameterization, which neglects spatial variability in land cover, soil properties, and slope. In addition, conventional CN values were developed under relatively mild topographic conditions and do not explicitly account for slope effects, which strongly influence runoff generation in steep terrain [8]. Furthermore, many studies assess LULC conditions at a single time period, limiting the ability to capture temporal variations in hydrological response. Recent studies have emphasized the need to integrate spatially distributed CN estimation, slope-adjusted modeling, and multi-temporal LULC analysis to improve the accuracy of runoff predictions [9, 10]. In addition, LULC change has been shown to significantly affect runoff generation and peak discharge, underscoring the importance of incorporating land cover dynamics into hydrological modeling [11, 12]. However, studies that simultaneously integrate land cover change, topographic variability, and spatially distributed hydrological modeling remain scarce, particularly in tropical mountainous Watersheds such as those in Indonesia [13].

A methodological gap exists in integrating: spatially distributed CN mapping derived from high-resolution LULC and soil datasets, slope-adjusted CN correction for mountainous terrain, and multi-temporal runoff and peak discharge simulation. In steep Watersheds, slope correction can be introduced by modifying CN as a function of terrain gradient:

$$CN_{adj} = CN_{II}\left(\frac{1+\beta \cdot Slope}{1+\gamma}\right) \tag{5}$$

where CN _represents standard curve number under normal moisture condition, and β and γ are empirical slope-adjustment coefficients.

Such engineering adaptation improves runoff estimation in complex terrain. For the Geuni Subwatershed, no prior study has systematically quantified changes in runoff depth and peak discharge from 2012 to 2022 using slope-adjusted spatial SCS–CN modeling. Therefore, quantitative evidence linking LULC transformation to discharge amplification in this mountainous system remains limited.

The Geuni Subwatershed offers a relevant case for investigating these interactions. Previous studies have shown that land cover change significantly affects infiltration and surface runoff [14], and research in Indonesian Watersheds has shown that LULC change influences runoff coefficients and flood hydrographs over time [15]. Applying hydrological models that incorporate land cover information is essential. The SCS-CN method, combined with spatial analysis, provides a practical framework for evaluating how land cover variations influence runoff depth and volume. Changes in CN values reflect shifts in land surface conditions, which directly affect runoff generation. Previous studies have shown that land-use change significantly alters environmental and hydrological conditions, further supporting the need for integrated analytical approaches [16]. However, these studies generally do not integrate slope effects and spatial variability within a unified modeling framework, indicating a gap in understanding the combined influence of land cover dynamics and terrain characteristics on runoff generation.

Therefore, this study aims to evaluate the hydrological impacts of land-cover change in the Geuni Subwatershed from 2012 to 2022 using an integrated, engineering-based approach. The objectives are: (1) to generate spatially distributed CN maps from LULC and soil data within a GIS framework, (2) to estimate runoff depth using a slope-adjusted SCS–CN method, (3) to simulate peak discharge using the SCS-UH method, and (4) to quantify changes in runoff and discharge associated with land-cover change.

This study advances hydrological modeling in mountainous environments by integrating spatial analysis, slope-adjusted runoff estimation, and multi-temporal land cover analysis. The proposed framework improves runoff prediction accuracy in data-limited regions and provides practical support for Watershed management and flood mitigation planning in the Krueng Meureudu Watershed and similar tropical mountainous systems [17].

II. METHODOLOGY

A. *Study Area*

This study was conducted in the upstream region of the Krueng Baroe Watershed, specifically in the Geuni Subwatershed, located at coordinates 5°11'28.5" N and 95°51'15.5" E in Tangse District, Pidie Regency, Aceh Province. Spatial data processing involved digitizing land cover in ArcGIS. Figure 1 presents the map of the Geuni Watershed.

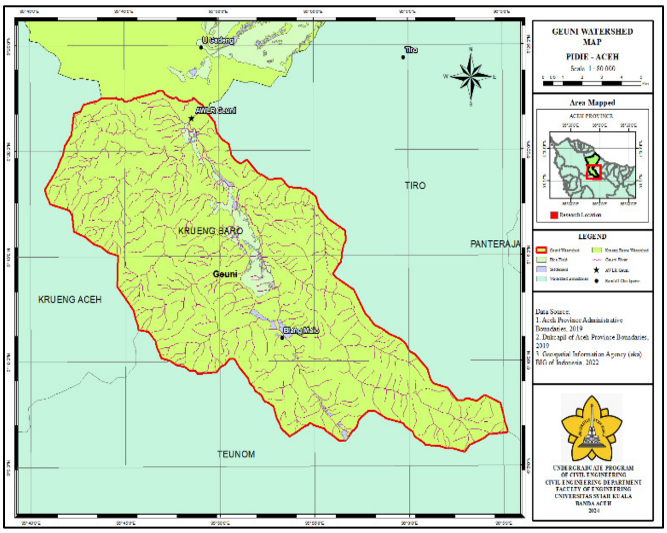

Fig. 1. The map of the Geuni Watershed.

B. *Methodology*

1) *Data Collection and Processing*

The data used in this study consisted of secondary data obtained from relevant institutions. The secondary data included rainfall data from nearby stations, land-cover maps for 2012, 2017, and 2022, soil type and hydrologic soil group (HSG) data, river network and Watershed boundary data, and Digital Elevation Model (DEM) data. Additional information on historical flood events and Watershed characteristics was also collected to support hydrological interpretation. Spatial data were analyzed in ArcGIS to identify land-cover changes and classify runoff coefficients. Rainfall data were analyzed to determine the design rainfall for hydrological modeling. All processed data served as input for the runoff discharge simulation.

2) *Model Development*

Hydrological modeling was conducted using the Soil Conservation Service (SCS) method to generate the design hydrograph under different land-cover conditions (2012, 2017, and 2022). The modeling process involved determining CN values based on land cover and soil type, estimating direct runoff, and generating peak flood discharge for different return periods. The analysis evaluated the effects of land-use change on runoff volume and peak discharge. The resulting hydrographs were compared across the three time periods to identify variations in flood-discharge trends associated with land-use changes.

3) *Model Validation*

Model validation in this study involves assessing the accuracy of flood discharge estimates from HEC-RAS simulations against field observations of flood events. The results of flood inundation simulations using HEC-RAS need to be validated to determine their representativeness. The validation of the simulation results is applied at the Geuni Village location using a discharge value of Q10 = 405.07 m³/s. This discharge value corresponds to the 2022 event, and the simulation results are examined to determine whether they produce flood inundation visualizations that correspond to field measurements according to Equation 6.

$$\Delta Q_{\text{flood}} = Q_{\text{flood model}} - Q_{\text{flood actual}} \tag{6}$$

Validation is the process of evaluating a model to assess its uncertainty in predicting flood events in the field. The validation value was evaluated using the Root Mean Square Error (RMSE), a metric that quantifies the difference between a model's predicted values and the observed values. The accuracy of the measurement error estimation method is indicated by a low RMSE.

The Root Mean Square Error (RMSE) is:

$$RMSE = \sqrt{\frac{\sum_{i=1}^{n}(y_i - \hat{y_i})^2}{n}} \tag{7}$$

where y_i is the observed value, $\hat{y_i}$ is the predicted value, and n is the number of data points.

4) Hydrology Analysis

Hydrological analysis was conducted to obtain the flood discharge hydrograph for the catchment area. This study employed the SCS Synthetic Unit Hydrograph (SCS-SUH) method to analyze flood discharge. For each sub-catchment, the input variables included CN, Watershed slope, Watershed area, and time-series rainfall intensity data with their return periods.

5) Spatial Analysis

The digitization and mapping processes were carried out using ArcGIS v10.5 for spatial analysis. The workflow included: (1) delineation of watershed boundaries, (2) land-cover classification, (3) extraction of land-cover information from satellite imagery, (4) development of a spatial database, (5) polygon digitization for area computation, and (6) determination of CN for hydrological modeling. The final output consisted of thematic land-cover maps and tabulated spatial statistics for each study year. Satellite imagery was obtained from Google Earth Pro, which provides mosaicked imagery compiled from multiple satellite and aerial sources. Medium-resolution datasets for earlier years are primarily derived from the Landsat missions, including Landsat 5, Landsat 7, and Landsat 8. The imagery resolution used in this study was 8192 × 4639 pixels. Although Google Earth Pro does not provide raw scientific raster formats, it allows consistent temporal visualization suitable for comparative land-cover interpretation.

Land-cover classification was performed through on-screen digitization of multi-temporal imagery (2012, 2017, and 2022). The time-slider function enabled temporal selection, and scale adjustment improved boundary delineation. Manual visual interpretation was used to ensure consistent land-cover identification across years. This approach served as an internal validation step by cross-checking spatial patterns and the morphological consistency of land features. Land cover was categorized into hydrologically relevant classes to support CN estimation under the SCS framework. The CN parameter was determined based on land-cover type and hydrologic soil group, and subsequently used to estimate effective rainfall.

Effective rainfall (P_e) was computed from total precipitation, accounting for initial abstraction and retention losses, following the standard SCS–CN formulation (8):

$$P_e = \frac{(P-0.2S)^2}{P+0.8S}, P > 0.2S \quad (8)$$

where P_e is effective rainfall (mm), P is total rainfall (mm), and S is the potential maximum retention (mm), which is derived from the CN.

The selected years (2012, 2017, and 2022) span a decadal period with five-year intervals. These years were selected for their data availability, consistent rainfall records, and hydrological relevance. Significant flood events in 2017 and 2022 in the Geuni Watershed enabled evaluation of the relationship between land-cover dynamics and flood response. Peak flood discharge was estimated using the SCS-SUH method. The model integrates effective rainfall, Watershed characteristics, and CN-derived parameters to generate design hydrographs. Computed peak discharge values for each study year were compared to assess temporal changes in hydrologic response. The correlation among land-cover change, CN variation, and simulated peak discharge was then analyzed to quantify the impact of Watershed dynamics on flood behavior.

III. RESULTS AND DISCUSSION

A. Watershed Characteristics

The upstream Subwatershed of the Krueng Baroe, known as the Geuni Watershed, covers an area of 167.66 km² and has a main river length of 28.76 km. The elevation at the river's upstream point is 537.5 meters, while the downstream elevation is 125, yielding a river slope of 0.014. Figure 2 presents the best available satellite imagery for 2012, 2017, and 2022.

(a) Year 2012

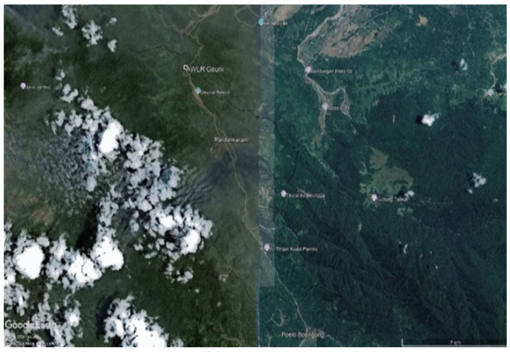

(b) Year 2017

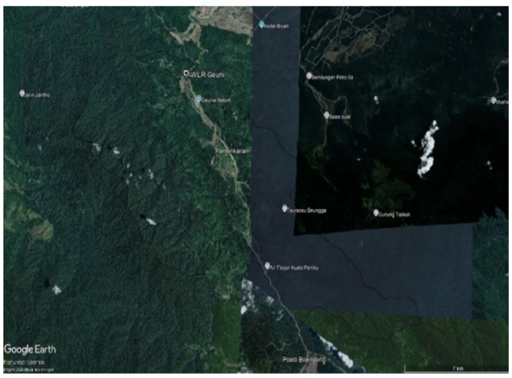

(c) Year 2022

Fig. 2. Satellite image maps of the Geuni Watershed for (a) 2012, (b) 2017, and (c) 2022. (c) Google Earth.

B. Land Cover

Based on the SNI 7645:2010 land-cover classification standards, the spatial analysis generated land-cover area data for 2012, 2017, and 2022, as shown in Figures 3, 4, and 5. These figures are scaled at 1:50,000 and use color coding: blue for water bodies, red for settlements, yellow for rice fields, green for open land, and cream for forests.

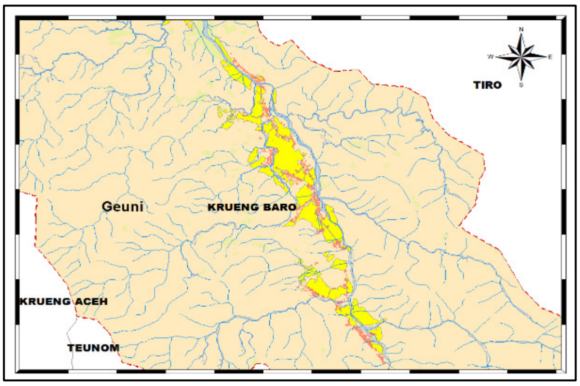

Fig. 3. Land-cover map of the Geuni Watershed for 2012.

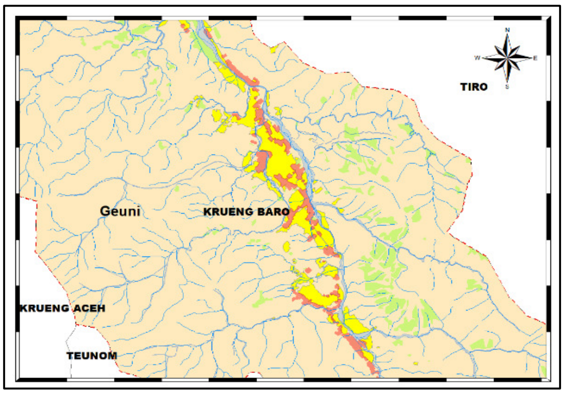

Fig. 4. Land-cover map of the Geuni Watershed for 2017.

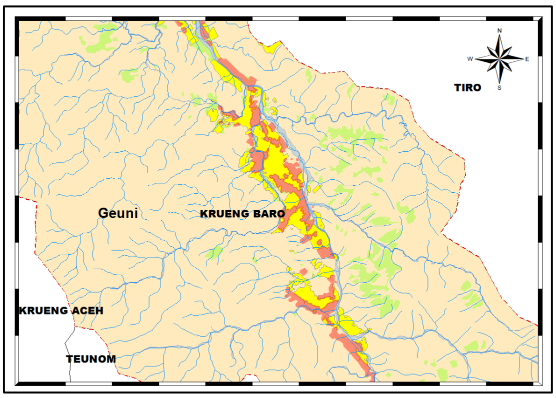

Fig. 5. Land-cover map of the Geuni Watershed for 2022.

Table I displays the land-cover areas, while Table II shows their respective percentages. Table I indicates that the area of settlements remains relatively small compared to other land uses. However, the settlement area has been expanding over time, driven by rising housing demand. This expansion occurs through the conversion of land previously designated as rice fields and open land. Conversely, rice fields cover a significant area and remain one of the dominant land uses, despite the conversion of only a small portion of their total area. In this study, open land includes spaces such as open fields, riverbanks, and forested areas without trees. The extent of open land has increased substantially over the years due to land conversion resulting from forest utilization. Tables I-II, Figure 6, and Figure 7 present the results of land-use analysis in the Geuni Watershed, showing significant changes in 2012, 2017, and 2022.

TABLE I. LAND-USE AREA (HA)

Land Type	Land Use Area (ha)		
	2012	2017	2022
Water Body	153.7	208.2	207.8
Settlements	56.0	162.8	248.9
Rice Fields	429.2	478.9	483.5
Open Land	256.8	473.9	538.8
Forest	15,870.2	15,442.2	15,287.0
Sum	16,766	16,766	16,766

TABLE II. LAND USE AREA RESULTS (%)

Land Type	Land Use Area (%)		
	2012	2017	2022
Water Body	0.92	1.24	1.24
Settlements	0.33	0.97	1.48
Rice Fields	2.56	2.86	2.88
Open Land	1.53	2.83	3.21
Forest	94.66	92.10	91.18
Sum	100	100	100

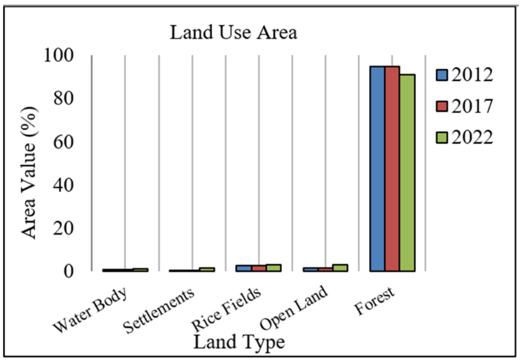

Fig. 6. Percentage of land use area of Geuni Watershed.

In 2012, forests covered 15,870.21 ha, or 94.66% of the total Watershed. Between 2012 and 2017, forest cover declined to 15,442.18 ha (92.10%), and it further decreased to 15,287.02 ha (91.18%) in 2022. Data from Walhi Aceh in 2017 reported that part of the Geuni Watershed falls within a protected forest and Other Land Uses (OLU).

This classification indicates that a substantial portion of the forest remains a crucial buffer for environmental sustainability and a source of livelihoods for development. Consequently, forest management within APL areas must prioritize conservation efforts. Other land types have increased in area. Water bodies (river channels) that originally covered only 153.71 ha (0.92%) have increased to 208.017 ha (1.24%) since

2017 and will remain at that level until 2022. Water bodies, such as rivers, are an important source of water for agricultural irrigation and community needs. Figure 8 illustrates the water body flow map.

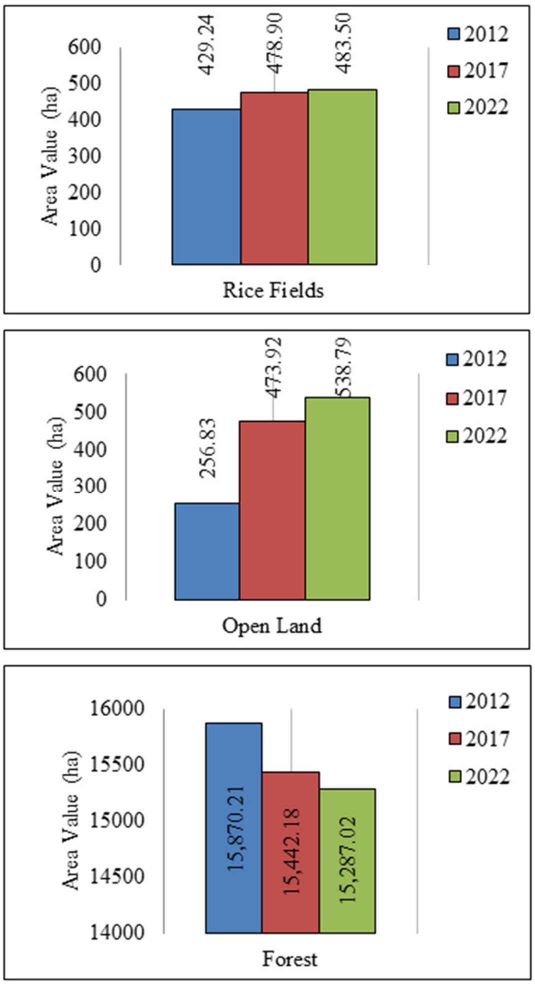

Fig. 7. Details of the land use area of the Geuni Watershed.

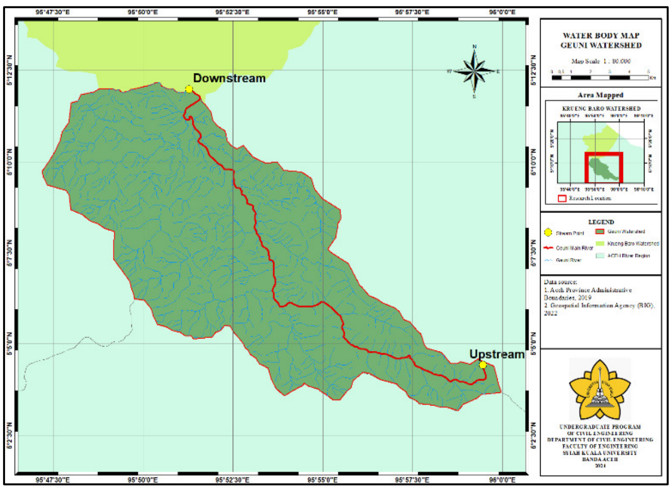

Fig. 8. Geuni Watershed map.

Settlements showed a substantial proportional increase, as illustrated in Figure 7, rising from 56.01 ha (0.33%) to 248.89 ha (1.48%) over a decade, primarily due to the conversion of paddy fields to residential use. Open land, initially covering 256.83 ha (1.53%), continued to expand, reaching 538.79 ha (3.21%) by 2022. In contrast, paddy fields changed relatively little, increasing from 429.24 ha (2.56%) to 483.50 ha (2.88%) over the same period, primarily due to the conversion of open land. Open land includes areas such as sports fields, cemeteries, and forests.

C. Rainfall Analysis

The influence area for each rainfall gauge station in the Geuni Watershed is as follows: ARR U Gadeng covers 46.71 km², Blang Malo covers 112.64 km², and Tangse covers 8.30 km². Figure 9 shows the spatial distribution of the rainfall gauge influence zones using the Thiessen Polygon method. Table III presents the results of the planned rainfall calculation using the Mononobe method and the Alternating Block Method. Td is the assumed duration of the rainfall event. The rainfall duration is assumed to be 6 hours.

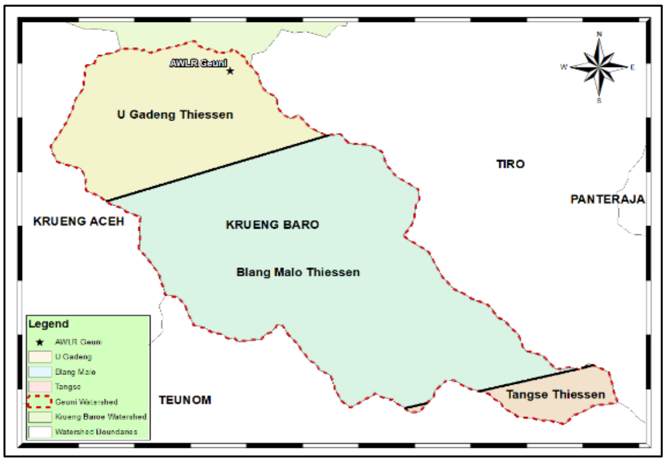

Fig. 9. Thiessen area rainfall map.

TABLE III. HYETOGRAPH OF THE PLANNED RAINFALL FOR A CERTAIN RETURN PERIOD OF THE ABM METHOD

Td	**Hyetograph 2-year**	**Hyetograph 5-year**	**Hyetograph 10-year**
(hour)	(mm)	(mm)	(mm)
1	8.06	11.01	12.29
2	11.99	16.38	18.28
3	65.76	89.83	100.26
4	17.09	23.35	26.06
5	9.54	13.04	14.55
6	7.05	9.62	10.74
	Hyetograph 25-year	**Hyetograph 50-year**	**Hyetograph 100-year**
	(mm)	(mm)	(mm)
1	13.37	13.90	14.28
2	19.88	20.68	21.24
3	109.06	113.42	116.51
4	28.35	29.48	30.28
5	15.83	16.46	16.91
6	11.68	12.15	12.48

In general, the highest rainfall occurs during longer return periods, with the peak value reached in the third hour. The effective rainfall hyetograph can be calculated using the SCS-CN method. The CN value is derived from the land-cover area, and the results are shown in Table IV.

TABLE IV. RECAPITULATION OF CURVE NUMBER

Year	CN composite
2012	65.63
2017	66.10
2022	66.27

The CN value affects the Watershed's physical ability to absorb rainfall. The higher the CN value, the greater the excess runoff from precipitation.

D. Base Flow Discharge

Temperature, humidity, wind speed, and sunshine duration data used in this study were obtained from BMKG (Meteorology, Climatology, and Geophysical Agency) Sultan Iskandar Muda, Blang Bintang, Aceh, at an elevation of 23 meters above sea level. The base flow values were initially recorded in millimeters and then converted to m³/s for discharge calculations. Table V summarizes a sample of these base flow calculations. As shown in Table V, the maximum base flow (BFmax) in 2012 is 94.26 mm, which corresponds to a discharge of 6.097 m³/s. For 2017 and 2022, the calculated discharges are 3.826 m³/s and 2.335 m³/s, respectively.

TABLE V. RELIABLE DISCHARGE IN 2012

Month	ET0	R	BF
	(mm/ month)		
Jan	83.68	27	60.00
Feb	81.19	29	94.26
Mar	91.93	22	12.21
Apr	91.02	32	32.20
May	99.76	14	44.75
Jun	115.66	16	52.67
Jul	115.23	5	45.31
August	110.24	26	44.56
Sept	106.50	12	43.20
Oct	93.50	27	49.38
Nov	82.66	28	49.18
Des	86.19	20	54.88
		Maximum BF	94.26

ET0 is evapotranspiration, R represents the average regional rainfall, and BF refers to baseflow.

E. Flood Discharge

The final results for peak flood discharge values across different return periods in each study year are presented in Table VI and Figure 11 displays the SCS hydrograph chart. As shown in Table VI, flood discharge increases gradually with increasing return periods. This trend is consistent with land-use changes that increase surface runoff in the Geuni Watershed. However, the magnitude of the increase is not substantially different among the study years, because CN values directly influence the SCS-UH calculations. As shown in Table IV, CN values remain relatively similar across all study years. Since the percentage of each land-cover class is calculated at the large-Watershed scale, the overall land-cover change appears limited, although land-use conversion may still be significant in absolute area. Complete slope-adjusted SCS–CN calculations for the Geuni Subwatershed, used as an example for the 2012–2022 period, are presented in Table VII.

TABLE VI. FLOOD DISCHARGE USING THE SCS HYDROGRAPH

T	2012		2017		2022		%Δ
	DR	Q_p	DR	Q_p	DR	Q_p	
year	m³/s						
2	140.92	147.02	144.03	147.86	145.16	147.49	0.32%
5	255.19	261.29	259.29	263.12	260.77	263.11	0.70%
10	308.48	314.58	313.00	316.83	315.65	317.98	1.08%
25	354.98	361.08	359.88	363.70	361.66	363.99	0.81%
50	378.66	384.75	383.76	387.59	385.60	387.93	0.83%
100	395.65	401.75	400.86	404.69	402.74	405.07	0.83%

T represents time or return period, DR stands for direct runoff, while Qp refers to the peak discharge, which is the sum of DR and Qbase (baseflow discharge), and %Δ indicates the percentage change in peak discharge from 2012 to 2022.

TABLE VII. COMPLETE SLOPE-ADJUSTED SCS–CN CALCULATION FOR THE GEUNI WATERSHED

Year	CN II	CN adj	S	Ia	P	R off Q	R off Vol	Qp
			mm	mm	mm	mm	m³	m³/s
2012	65.63	50.66	247.37	49.47	89.83	5.66	949.02	65.80
2017	66.10	51.02	243.80	48.76	100.26	8.98	1505.79	104.40
2022	66.27	51.16	242.53	48.51	109.06	12.10	2028.45	140.64

The Synthetic Unit Hydrograph using the SCS method (HSS–SCS) was used to estimate direct runoff hydrographs for different return periods, as shown in Figures 10–12.

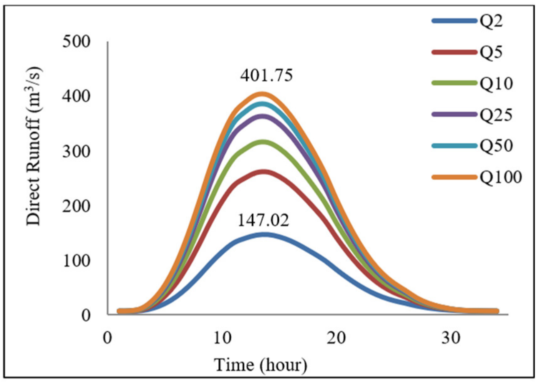

Fig. 10. HSS–SCS direct runoff hydrographs for 2012.

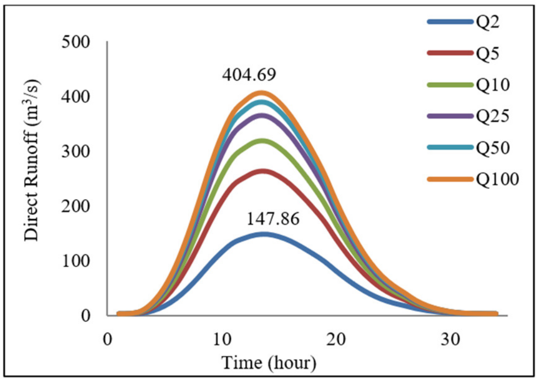

Fig. 11. HSS–SCS direct runoff hydrographs for 2017.

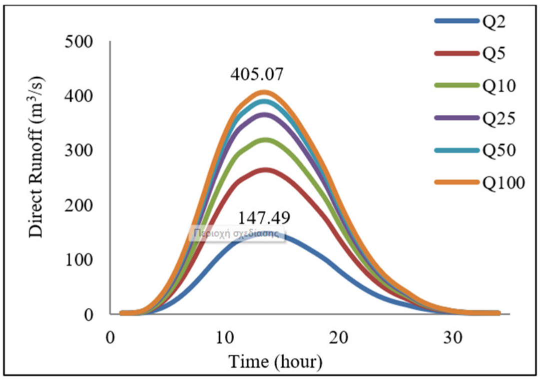

Fig. 12. HSS–SCS direct runoff hydrographs for 2022.

1) Complete Slope-Adjusted SCS–CN Calculation for the Geuni SubWatershed (Example of Research Calculations 2012–2022)

The slope-adjusted SCS–CN calculation was applied to the Geuni Subwatershed for the period 2012–2022. The calculation procedure included estimating CN, runoff depth, and peak discharge using Watershed parameters derived from GIS analysis, such as rainfall, slope, Watershed area, and slope-correction factors. The resulting CN, runoff depth, and peak discharge values for each year are presented in Table VIII.

TABLE VIII. CHANGE ANALYSIS 2012–2022

Year	CN	Runoff (mm)	Qp (m³/s)
2012	50.66	5.66	65.798
2017	51.02	8.98	104.401
2022	51.16	12.099	140.639

Overall, the results indicate that land-cover changes during 2012–2022 were associated with increased CN values, runoff depth, and peak discharge in the Geuni Watershed.

2) Validation of Flood Events in the Geuni Watershed (2012–2022)

Flood events in the Geuni Watershed (DAS Geuni), a sub-basin of the Meureudu Watershed (DAS Meureudu) in Pidie Jaya, show a progressive increase in severity and spatial impact from 2012 to 2022. In 2012, flooding occurred during the peak rainy season due to high-intensity rainfall. However, the inundation was relatively localized, with limited spatial coverage and shorter flood duration. The hydrological response was mainly driven by seasonal rainfall, with no extreme cumulative precipitation. In 2017, flood events were more intense than in 2012, particularly during extreme rainfall episodes. Surface runoff increased because of reduced infiltration capacity and ongoing land-use changes in the upstream area. Although flood depth and the number of affected settlements increased, the impacts remained moderate and did not reach catastrophic levels. The 2022 flood event is included in the three-year comparison. Prolonged extreme rainfall triggered significant river overflow, causing widespread inundation in downstream areas of the Geuni Subwatershed. The severity was exacerbated by watershed degradation, reduced vegetation cover, and limited channel capacity. Compared to 2012 and 2017, the 2022 event exhibited: higher rainfall accumulation, larger inundation extent, longer flood duration, and greater socioeconomic impact. Overall, validation of historical flood records confirms that flood intensity and impact in the Geuni Watershed have increased over time. The 2022 event reflects a combination of extreme hydrometeorological conditions and declining Watershed resilience, indicating a growing trend in flood risk in the basin.

IV. CONCLUSION

Over the past decade, land-cover changes in the Geuni Watershed have been characterized by a 344% increase in settlement areas (from 56.01 ha to 248.89 ha) and a 110% increase in open land (from 256.83 ha to 538.79 ha). In contrast, forest cover declined slightly from 94.66% to 91.18% of the total Watershed area. Correspondingly, the modeled peak flood discharge showed only a modest rise, increasing by approximately 0.3% for the 2-year return period and 0.8% for the 100-year return period. This study evaluated the hydrological response of the Geuni Subwatershed using the Soil Conservation Service Curve Number (SCS–CN) method integrated with slope correction and GIS-based spatial analysis. The analysis was conducted to assess the impact of land use changes between 2012 and 2022. The results showed that land use changes significantly affected the hydrological characteristics of the Watershed. The conversion of forest areas to agricultural land and settlements increased the composite Curve Number, resulting in higher runoff depth and volume. The slope-adjusted Curve Number method provided a more realistic representation of runoff generation under steep Watershed conditions than the standard SCS–CN approach.

The analysis indicated that runoff depth, runoff volume, and peak discharge increased from 2012 to 2022, indicating that the watershed's hydrological response has become more sensitive to rainfall events. The rise in peak discharge suggests a higher potential flood risk in the watershed, particularly during high-intensity rainfall events. Integrating slope correction into the SCS–CN model improved runoff estimation in mountainous tropical watersheds and can be applied to ungauged watersheds with limited hydrological data. This approach provides useful information for watershed management, flood mitigation planning, and land use planning.

Overall, land use change and terrain slope are key factors influencing runoff generation in the Geuni Subwatershed, and proper Watershed management is necessary to reduce runoff and flood risk in the future. Flood events in the Geuni Watershed, a sub-basin of the Meureudu Watershed, are strongly influenced by interactions among land cover change, Watershed morphology, and rainfall intensity. Steep slopes, reduced infiltration capacity, and the conversion of vegetated land to agricultural and settlement areas have accelerated surface runoff and increased peak discharge during high-intensity rainfall events. Hydrological analysis indicates that land cover changes have increased runoff coefficients and Curve Number (CN) values, resulting in greater direct runoff and higher flood risk within the Watershed system. The results show that flooding in the Geuni Watershed is driven not only by extreme rainfall but also by anthropogenic land-use changes that reduce infiltration and storage capacity. Therefore, effective flood mitigation requires integrated Watershed management that combines structural and non-structural measures. These measures include reforestation of critical upstream areas, soil and water conservation practices, improved land-use planning, river channel rehabilitation, and the implementation of eco-hydrological approaches, such as riparian vegetation restoration.

Controlling the destructive power of floods and droughts is one strategy for managing existing water resources [17]. Overall, sustainable watershed management in the Meureudu basin is essential for reducing peak discharge, enhancing infiltration capacity, and improving long-term hydrological resilience. The integration of Nature-based Solutions (NbS) is recommended as a sustainable strategy to restore natural watershed functions and strengthen flood resilience. In addition, eco-hydraulic approaches, such as planting large trees and restoring riparian vegetation, can significantly improve infiltration and reduce flood peaks [18]. Implementing NbS can restore the natural condition of the environment to its original state. The application of NbS aims to improve flood resilience, including in urban areas.

DECLARATION OF COMPETING INTERESTS

The authors declare that they have no financial or personal relationships that may have inappropriately influenced them in writing this article.

ACKNOWLEDGEMENTS

The authors thank the Irrigation Service, River Basin Office, and the Regional Disaster Management Agency for their assistance in field data acquisition.

DATA AVAILABILITY

The data that support the findings of this study are available from the corresponding author upon reasonable request.

FUNDING INFORMATION

This research was conducted with support from the Research and Community Services Institute, Universitas Syiah Kuala.

REFERENCES

[1] D. Viviroli *et al.*, "Climate change and mountain water resources: overview and recommendations for research, management and policy," *Hydrology and Earth System Sciences*, vol. 15, no. 2, pp. 471–504, Feb. 2011, https://doi.org/10.5194/hess-15-471-2011.

[2] S. S. Dash, B. Naik, and P. S. Kashyap, "Assessment of land use/ land cover change derived catchment hydrologic response: An integrated parsimonious hydrological modeling and alteration analysis based approach," *Journal of Environmental Management*, vol. 356, Apr. 2024, Art. no. 120637, https://doi.org/10.1016/j.jenvman.2024.120637.

[3] K. Gabriels, P. Willems, and J. Van Orshoven, "A comparative flood damage and risk impact assessment of land use changes," *Natural Hazards and Earth System Sciences*, vol. 22, no. 2, pp. 395–410, Feb. 2022, https://doi.org/10.5194/nhess-22-395-2022.

[4] K. Z. Besha, T. A. Demissie, and F. F. Feyessa, "Effects of land use/land cover change on hydrological responses of a Watershed in the Central Rift Valley of Ethiopia," *Hydrology Research*, vol. 55, no. 2, pp. 83–111, Jan. 2024, https://doi.org/10.2166/nh.2024.042.

[5] *SCS National Engineering Handbook*, Washington, DC, USA: U.S. Department of Agriculture, Soil Conservation Service, 1985.

[6] S. K. Mishra and V. P. Singh, *Soil Conservation Service Curve Number (SCS-CN) Methodology*, Water Science and Technology Library, vol. 42. Dordrecht, The Netherlands: Springer, 2003, https://doi.org/10.1007/978-94-017-0147-1.

[7] M. Rizalihadi, Z. Ziana, N. Shaskia, and H. Asharly, "The effect of ratio between rigid plant height and water depth on the manning's coefficient in open channel," *IOP Conference Series: Materials Science and Engineering*, vol. 352, no. 1, Feb. 2018, Art. no. 012039, https://doi.org/10.1088/1757-899X/352/1/012039.

[8] A. Panigrahi and M. Ramadas, "Revisiting the Curve Number Approach for Improving Surface Runoff Estimation: A State-of-the-Art Review," *Journal of Irrigation and Drainage Engineering*, vol. 151, no. 4, Aug. 2025, Art. no. 03125001, https://doi.org/10.1061/JIDEDH.IRENG-10173.

[9] S. Verma and R. K. Verma, "SCS-CN methodology further modified," *Water Supply*, vol. 23, no. 6, pp. 2604–2622, May 2023, https://doi.org/10.2166/ws.2023.129.

[10] W. Shi and N. Wang, "An Improved SCS-CN Method Incorporating Slope, Soil Moisture, and Storm Duration Factors for Runoff Prediction," *Water*, vol. 12, no. 5, May 2020, Art. no. 1335, https://doi.org/10.3390/w12051335.

[11] A. Yono, R. A. Mokua, and T. Dube, "Remote sensing of land cover change dynamics in mountainous catchments and semi-arid environments: a review," *Geocarto International*, vol. 40, no. 1, Mar. 2025, Art. no. 2476602, https://doi.org/10.1080/10106049.2025.2476602.

[12] M. Banjara, A. Bhusal, A. B. Ghimire, and A. Kalra, "Impact of Land Use and Land Cover Change on Hydrological Processes in Urban Watersheds: Analysis and Forecasting for Flood Risk Management," *Geosciences*, vol. 14, no. 2, Feb. 2024, Art. no. 40, https://doi.org/10.3390/geosciences14020040.

[13] L. Dwivedi, R. Pandey, and S. Tripathi, "Remote sensing and GIS based morphometric characterization of Bichiya river Watershed of Rewa district, MP," *International Journal of Applied Research*, vol. 8, no. 6, pp. 101–107, June 2022, https://doi.org/10.22271/allresearch.2022.v8.i6b.9829.

[14] J. M. Hassen, "Understanding the Impact of Land Use and Land Cover Change on Local Hydrology: Implications for Long-Term Planning in the Sore and Geba Watersheds, Southwestern Ethiopia," *Open Access Library Journal*, vol. 9, no. 2, pp. 1–16, Feb. 2022, https://doi.org/10.4236/oalib.1108161.

[15] P. Irawan and J. Setiawan, "Forecasting the long-term impacts of land use and cover changes on runoff coefficient and flood hydrograph: a case study of the Upper Citanduy Basin, Indonesia," *Journal of Degraded and Mining Lands Management*, vol. 12, no. 3, pp. 7417–7429, Apr. 2025, https://doi.org/10.15243/jdmlm.2025.123.7417.

[16] J. Sudrajat, A. Suyatno, and S. Oktoriana, "Land-Use Changes and Food Insecurity around Oil Palm Plantations: Evidence at the Village Level," *Forest and Society*, vol. 5, no. 2, pp. 352–364, July 2021, https://doi.org/10.24259/fs.v5i2.11376.

[17] R. Karamma, S. Badaruddin, M. R. Mustamin, and M. I. Mukrim, "Flood Risk Assessment and Mitigation Strategies for the Sinjai and Tangka River Catchments in Indonesia using Hydraulic Modeling and Spatial Analysis," *Engineering, Technology & Applied Science Research*, vol. 15, no. 2, pp. 20623–20634, Apr. 2025, https://doi.org/10.48084/etasr.9837.

[18] Z. Ziana, A. Azmeri, A. Yulianur, and E. Meilianda, "The eco-hydraulics base as flood mitigation to overcome erosion and sedimentation problems: A case study in the Lae Kombih River, Indonesia," *Journal of Water and Land Development*, no. 55, pp. 229–239, Dec. 2022, https://doi.org/10.24425/jwld.2022.142326.